# Automated Parameter Extraction Software for Silicon and High-Voltage Silicon Carbide Power Diodes

Nanying Yang[1, 2], Tam Duong[2], Jeong-O Jeong[1†], Jose M. Ortiz[2], Allen Hefner[2], Kathleen Meehan[1]

[1]Bradley Department of Electrical and Computer Engineering, 476 Whittemore Hall, Virginia Tech
Blacksburg, VA 24060, USA
Email: nyang06@vt.edu

[2]National Institute of Standards and Technology[+]
Semiconductor Electronics Division
100 Bureau Dr., Stop 8120
Gaithersburg, MD 20899

*Abstract*— **This paper presents an automated parameter extraction software package developed for constructing silicon (Si) and silicon carbide (SiC) power diode models, which is called DIode Model Parameter extrACtion Tools (DIMPACT). This software tool extracts the data necessary to establish a library of power diode component models and provides a method for quantitatively comparing between different types of devices and establishing performance metrics for device development. To verify the accuracy of DIMPACT, the extracted model parameter sets are incorporated into the circuit simulation software to compare model predictions with measured static and transient diode characteristics. In this paper, the DIMPACT parameter extraction results are demonstrated for a 45 V, 15 A Si Schottky diode; a 600 V, 200 A Si PiN diode; a 10 kV, 5 A SiC Junction Barrier Schottky (JBS) diode; and a 10 kV, 20 A SiC PiN diode. The validation results indicate that the model parameters extracted using DIMPACT are accurate.**

*Keywords: Power diodes, SiC, parameter extraction.*

## I. INTRODUCTION

A wide range of diodes are currently available to fulfill the needs of various applications. Furthermore, new diodes are being developed and introduced that take advantage of advanced semiconductor materials (e.g., SiC) and advanced internal device structures. In order for circuit designers to perform a system-level simulation, compact models for these devices are needed in circuit and system simulation tools. Such tools provide a means to select appropriate device types for a given application and to optimize circuit performance, provided that accurate models can be readily produced from measured device characteristics. The purpose of this paper is to introduce an automated software package called DIode Model Parameter extrACtion Tools (DIMPACT) that enables rapid development and validation of device component models in Saber[*] for various types of Si and SiC power diodes.

This new software tool provides a method to extract the necessary modeling parameters for four classes of power diodes: (a) Schottky diodes, which offer high switching speed but suffer from high leakage current; (b) PiN diodes, which offer low leakage current but suffer from slow reverse recovery switching characteristics; (c) Junction barrier Schottky (JBS) diodes, which take advantage of p-n grids and offer low leakage current; and (d) Merge PiN Schottky (MPS) diodes, which combine the advantages of Schottky and PiN diodes to offer Schottky-like on-state and switching characteristics and PiN-like off-state characteristics [1].

In this paper, extraction and validation results are presented for (a) 15 A, 45 V Si Schottky diode, (b) 200 A, 600 V Si PiN diode, (c) 5 A, 10 kV SiC JBS diode [2], and (d) 20 A, 10 kV SiC PiN diode. The device models constructed using the extracted parameters from DIMPACT are validated for both static and transient characteristics. The 45 V Si Schottky diode and the 10 kV SiC JBS diode are employed in the DARPA High Power Electronics (HPE) Phase III program [3]. The 600 V Si PiN diode is used in parallel with the main IGBT switch in high efficiency soft-switching inverters for electric vehicle motor drives [4].

## II. POWER DIODE MODEL DESCRIPTION

The model equations of the forward-bias, reverse recovery, and temperature dependence implemented in DIMPACT are based on the Mantooth-Duliere unified diode model due to its efficiency. It is currently available in Saber. Temperature-dependent material properties of 3C-, 4H-, and 6H-SiC were added to the diode model as an enhancement [5, 6]. This paper presents a further enhancement to the diode model to better model the reverse blocking characteristics by including the thermionic emission leakage current in the low-bias range, which makes the new model more accurate.

### A. Static Characteristics

Because the unified diode model used in DIMPACT can be used to model a wide variety of diodes, it includes more effects in the generic diode model than would be typically required to characterize any particular diode.

### 1). Forward-Bias Operating Region

The unified model possesses the most elaborate dc effects commercially available [7]. The most widely known form of the diode equation

$$i = I_S \cdot \left( e^{\frac{V_j}{N \cdot V_T}} - 1 \right) \tag{1}$$

where $I_S$ is the saturation current, $V_j$ is the forward diode junction voltage, N is the emission coefficient, and $V_T$ is the thermal voltage, is used for depletion region recombination (ISR, NR) and emitter or end region recombination (ISE, NE). Equations similar to (1) are also used for the high- and low-level base injection currents, unless both conditions apply; then the equations are coupled to provide better continuity and flexibility in characterization

$$i_0 = \frac{2i_L}{1 + \left[1 + \left(2\frac{ISL}{ISH}\right)^{N_{eff}} e^{V_j/V_T}\right]^{1/N_{eff}}} \quad (2)$$

where

$$Neff = \frac{1}{\frac{1}{NL} - \frac{1}{NH}}. \quad (3)$$

In (2), $i_L$ is the low level injection current that takes the form of (1), and ISL, ISH, NL, and NH are the saturation currents for the low- and high-level injection regions and the corresponding emission coefficients, respectively. Each current component's saturation current $I_S$ is also a function of temperature. Their relationships have the following form:

$$I_S(T) = I_S(TNOM) \cdot \left(\frac{T}{TNOM}\right)^{XTI} \cdot e^{\left[\left(\frac{T}{TNOM}\right) - 1\right]\left(\frac{EG}{N \cdot VT}\right)} \quad (4)$$

where XTI is the saturation current temperature exponent for each current component, and N is the temperature dependent emission coefficient for each current. The emission coefficient of each current component has a temperature dependence given by

$$N(T) = N(TNOM) \cdot \left[1 + TN1 \cdot (T - TNOM) + TN2 \cdot (T - TNOM)^2\right] \quad (5)$$

where TN1 and TN2 are the linear and quadratic temperature coefficients for each current component.

The temperature dependence of the forward series contact resistance, $R_S$, implemented to provide greater flexibility in describing the series resistance due to the device and package effects, is given by

$$R_S(T) = R_S(TNOM) \cdot \left[\left(\frac{T}{TNOM}\right)^{GAMMA} + \right.$$
$$\left. TRS1 \cdot (T - TNOM) + TRS2 \cdot (T - TNOM)^2\right] \quad (6)$$

where $\gamma$, or GAMMA, is the exponential temperature parameter, TRS1 is the linear temperature parameter, and TRS2 is the quadratic temperature parameter.

*2). Reverse-Bias Operating Region*

In the current power diode model in the Saber circuit simulator, an empirical approach was used to describe the low-bias reverse blocking region by introducing an effect called "conduction loss," a parameter that causes a linear relationship between the device voltage and current at low bias voltages with no physics meaning [7]. Furthermore, this term is not sufficient to accurately describe the changes to the device characteristics as the junction temperature is varied. A more accurate model is required in order to adjust different systems, to fine tune the parameters of the energy management system,

and to design power electronics system [8]. In this paper, a new physics-based model of the reverse blocking characteristics for power Schottky/JBS diodes was developed by including the thermionic-emission mechanism in the low-bias range and was implemented in the Saber circuit simulator as an enhancement to the current power diode model.

According to the thermionic-emission theory [9], the reverse leakage current of a Schottky diode can be expressed by

$$I_{th} = A \cdot A^* T^2 e^{-\frac{(\Phi_{B0} - \Delta\Phi_B)}{kT}} \quad (7)$$

where $A^*$ is the effective Richardson constant, $\phi_{B0}$ is the zero-biased Schottky barrier height, and $\Delta\phi_B$ is the lowering of the barrier height given by [9]

$$\Delta\Phi_B = q\left[\frac{q|E|}{4\pi\varepsilon}\right]^{1/2}. \quad (8)$$

In (8), $E$ represents the internal electric field at the Schottky contact written in the form of

$$E = \sqrt{\frac{qN_d}{2\varepsilon}\left(V_R + \psi_{bi} - \frac{kT}{q}\right)} \quad (9)$$

where $N_d$ is the background doping concentration, and $\Psi_{bi}$ is the junction build-in voltage. The equation for pre-avalanche breakdown impact ionization effect is an exponential relationship adopted from the current power diode model in the form of

$$I_i = X_{BV} \cdot \left(e^{-(V_j + BV)/(N_{BV} \cdot V_T)} - e^{-BV/(N_{BV} \cdot V_T)}\right) \quad (10)$$

where BV is the breakdown voltage, $N_{BV}$ is a fitting parameter, and

$$X_{BV} = \frac{I_{BV} - I_{th}}{e^{\frac{V_j + BV}{N_{BV} \cdot V_T}} - e^{\frac{BV}{N_{BV} \cdot V_T}}} \quad (11)$$

where $I_{BV}$ is the current at breakdown voltage.

The JBS diode is a Schottky diode structure with a p-n junction grid integrated into its drift region. When the reverse bias exceeds certain voltage, the depletion layer become pinched-off and a potential barrier is formed in the channel. The reverse leakage current of a JBS diode can be expressed by

$$I_{th} = R \cdot A \cdot A^* T^2 e^{-\frac{(\Phi_{B0} - \Delta\Phi_B)}{kT}} \quad (12)$$

where R is a ratio parameter related to the window area and mask region of the p-n grids as well as structural dimensions [9]. Ideally, once the neck region becomes pinched-off, the electric field at the Schottky contact remains constant (independent of the reverse-bias voltage). Hence, the leakage current from the thermionic-emission should not change with the increase of the reverse-bias voltage ($V_R$). However, it is reported that instead of being constant after pinch-off, the electric field at the Schottky contact is still changing with $V_R$ but raised to a different power [10]. Thus, for JBS diodes the internal electric field can be described as

$$E = \left[ \frac{qN_d}{2\varepsilon} \left( V_R + \psi_{bi} - \frac{kT}{q} \right) \right]^{\alpha} \tag{13}$$

where $\alpha$ is introduced as the fitting parameter for the electric field at the Schottky contact. The equation for the pre-avalanche breakdown impact ionization effect is the same as the one used for conventional Schottky diodes as shown in (10).

Parameters BV, $I_{BV}$, and $N_{BV}$ have already been defined in the present Saber model [7]. Among the parameters that evolved in the new enhanced model, $\phi_{B0}$ (or BH0) is varied according to temperature in the form of

$$\phi_{B0}(T) = \phi_{B0}(TNOM) \cdot [1 + T\phi_{B0}1 \cdot (T - TNOM) + T\phi_{B0}2 \cdot (T - TNOM)^2] \tag{14}$$

where $T\Phi_{B0}1$ (or TBH01) and $T\Phi_{B0}2$ (or TBH02) are the linear and quadratic temperature coefficients for $\phi_{B0}$ (or BH0). Here $\alpha$ varies with temperature according to

$$\alpha(T) = \alpha(TNOM) \cdot [1 + T\alpha1 \cdot (T - TNOM) + T\alpha2 \cdot (T - TNOM)^2] \tag{15}$$

where $T\alpha1$ and $T\alpha2$ are the linear and quadratic temperature coefficients for $\alpha$. All the model parameters employed in the new model can be extracted automatically using DIMPACT. Details of the extraction sequence will be described in section III.

In Fig. 1, a comparision between the measured data, the simulated curves of the new enhanced model, and the simulated curves of the current model are shown for the 10 kV SiC JBS diodes at 125 °C. At 1 kV, excellent agreement between the measured data and the simulated curve using the new model is obtained. On the other hand, the error between the measured data and the simulated curve using the old model has been found to be 27 %. It is obvious that this new model will allow the validation of system behavior with a high degree of accuracy under the reverse blocking condition, especially for most of the low-bias range.
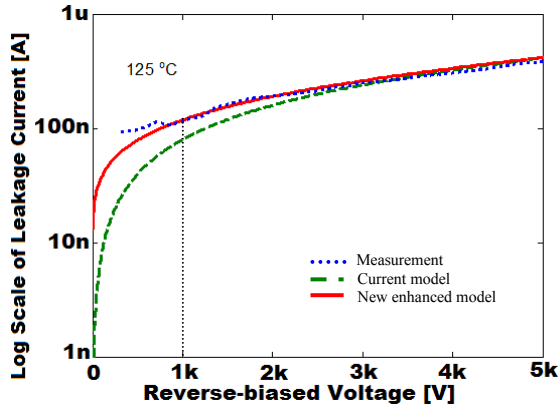


**Fig. 1** Comparison between measured data (dotted line), simulated curve of current model (dashed line), and simulated curve of new enhanced model (solid line) for the 10 kV SiC JBS diode at 125 °C in the low bias range.

### B. Transient Characteristics

Beyond the static characteristics, model equations for the transient characteristics (reverse recovery and capacitance-voltage) are also implemented in DIMPACT in order to extract the dynamic parameters including the zero-bias junction capacitance ($C_{J0}$), the package capacitance ($C_P$), the base charge decay parameter (TT), the charge sweep out time (TSW), and the mid-region recombination time (TM). TT, TSW, and TM can be varied according to temperature through relationships of the form

$$TT(T) = TT(T_{nom}) \cdot \left( \frac{T}{T_{nom}} \right)^{\beta} \tag{15}$$

where each time constant possesses a unique $\beta$ and the model parameters are defined at a nominal temperature, $T_{nom}$ [7].

For Schottky diode technologies, the lack of stored charge reduces the reverse recovery to that of charging the depletion and package capacitances [5]. Once the diode current crosses zero, the voltage rises as the diode depletion capacitance and package capacitance are charged. The initial reverse recovery current peak is due to the junction capacitance, while the further increase in the negative reverse current as the diode voltage rises is due to the package capacitance current. Hence, the values for $C_{J0}$ and $C_P$ should be extracted such that the corresponding voltage waveforms are aligned and have the correct dv/dt. Capacitance-voltage measurement is another method to extract $C_{J0}$ by reading the capacitance value at zero-bias voltage.

For PiN diodes, the dynamic parameters are extracted from reverse recovery measurements for low current and low dv/dt. Extracting the dynamic parameters at low current ensures the emitter recombination current is at a minimum, and, by reducing the dv/dt seen by the diode, the package and junction capacitance currents are reduced leaving only the decay of the stored charge. TT is extracted from the maximum reverse current and the decay of the tail current after turnoff. TSW is extracted during the first phase, and TM is extracted during the second phase of the tail current decay [5].

### III. PARAMETER EXTRACTION USING DIMPACT

The DIMPACT software package consists of three programs: JBSMSR (Junction Barrier Schottky MeaSuRement), MPSMSR (Merge PiN Schottky MeaSuRement), and PiNMSR (PiN MeaSuRement) as shown in Fig. 2 (a). The JBSMSR and MPSMSR programs enable parameter extraction from measurements of forward conduction (**Forward IV**), **Reverse Recovery**, capacitance-voltage (**CV**), and **Reverse Leakage** as shown in Fig. 2 (b). The PiNMSR program enables parameter extraction from measurements of forward conduction (**Forward IV**) and **Reverse Recovery**. Since the extraction techniques developed for Schottky and JBS power diodes are equally applicable to MPS power diodes that are operated in the junction-barrier-controlled-Schottky mode as discussed in [5], they share the same sets of model parameters. Consequently, the JBSMSR program and the MPSMSR program were combined to share the same technical parameter extraction procedure and

software interface of **Forward IV** and **Reverse Recovery** as shown in Fig. 2 (a). The detailed model parameter extraction sequence will be described for the combined JBSMSR/MPSMSR program in subsection A and for the PiNMSR program in subsection B.

### A. JBSMSR/MPSMSR Program

By selecting "JBSMSR" from the drop-down list as shown in Fig. 2 (a) and selecting the "RUN" button, a pop-up sub-panel shown in Fig. 2 (b) will used to select extraction from measurements listed as **Forward IV**, **Reverse Recovery**, **CV**, and **Reverse Leakage**. Details of each extraction are presented in sequence in the following subsections:
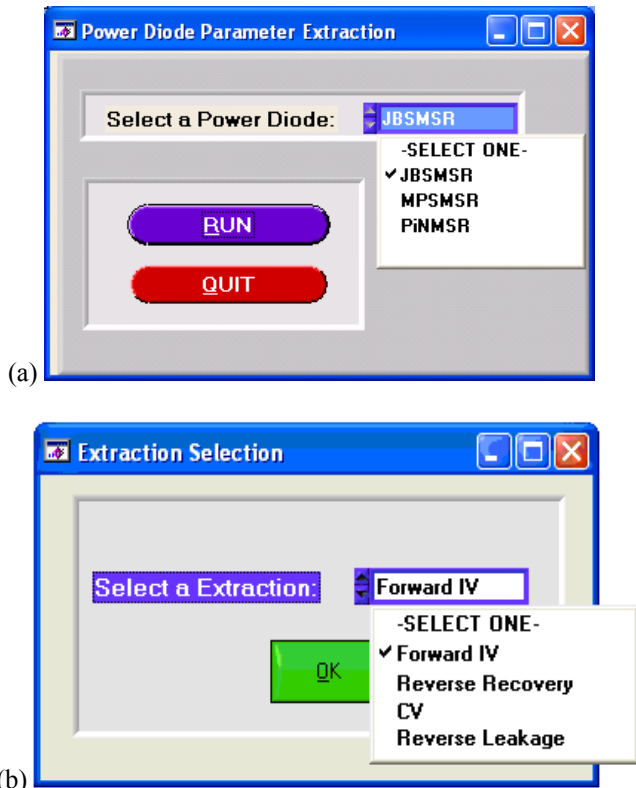


(a)



(b)

**Fig. 2** (a) DIMPACT front panel of program; (b) Pop-up panel of Schottky/JBSMSR program

#### 1). Forward IV

Fig. 3 shows the sub-panel of the parameter extraction program (**Forward IV**/**Reverse Recovery**) selected from the drop-down list as shown in Fig. 2 (b). The top half of the sub-panel was designed for the parameter extraction program of **Forward IV**, which is capable of extracting all the model parameters used in the forward-bias region including ISR, NR, XTIR, $V_J$, $R_S$, TNR1, TNR2, TRS1, TRS2, and GAMMA. These parameters are shown in the parameter list on the far right side of Fig. 3 as they are extracted.

The extraction sequence begins with the selection of the semiconductor material type as well as the test fixture temperature. By selecting the "ADD" button, the extraction temperature will be loaded into the table located in the middle of the Fig. 3. To perform the extraction, the anode diode current is measured as a function of the anode-cathode diode

voltage at temperatures from 25 °C to 175 °C. Two commercial semiconductor curve tracers are used to aid in the parameter extraction process. The upper-left graph of Fig. 3 shows diode current versus diode voltage on a logarithmic scale for the low-current range, which is used to extract parameters ISR, NR, and XTIR. The measurement is performed using the low-power curve tracer which can measure down to 1 μA. The measured data is loaded into the graph using the "File" pull-down menu by selecting the "Load Low LN Curve" option from the "Load" submenu. The upper-right graph shows the diode current versus diode voltage for the high-current range, which is used to extract parameters $V_J$ and $R_S$. The measurement is performed using the high-power curve tracer with power up to 3 kW. The measured data are loaded into the graph using the "File" pull-down menu by selecting the "Load single IV curve" option from the "Load" submenu. Here, the user should make sure that the data loaded for each extraction correspond to the test fixture temperature highlighted in the table.

The extraction of the parameters at each temperature is performed as follows: the first step is to extract the low current parameters including ISR, NR, and XTIR. By placing the two cursors in the linear region of the low current logarithmic graph (on the left-hand side) and selecting the "EXTRACT" button, the program will find the *y-intercept* and *slope* that are used to extract the initial values for ISR and NR as shown in (1). The extraction results for ISR, NR, and XTIR are displayed in the orange columns. The second step is to extract the high-current parameters including $V_J$ and $R_S$ using the already extracted values of ISR, NR, and XTIR. This is performed by placing the two cursors in the linear region of the high-current level graph (on the right-hand side) and selecting the "$V_J$" button and then selecting the "$R_S$" button to refine the values of ISR, NR, and XTIR. The program then guides the user back through this process iteratively by performing these two steps to optimize the static parameters for the full current range.

The temperature-dependent coefficients or exponents can be extracted after repeating the extraction procedure for each measurement temperature. By taking the natural logarithm of both sides of (4) [7], it can be written as

$$XTIR = \frac{\ln\left(\frac{ISR(T)}{ISR(TNOM)}\right) - \left[\left(\frac{T}{TNOM}\right) - 1\right] \cdot \left(\frac{EG}{NR \cdot VT}\right)}{\ln\left(\frac{T}{TNOM}\right)} \quad (16)$$

in order to extract XTIR. Equation (5) is used to extract TNR1 and TNR2 by using the Linear Equation Method as shown in the following matrix equation:

$$\begin{pmatrix} \frac{N(T_1)}{N(T_{nom})} - 1 \\ \bullet \\ \bullet \end{pmatrix} = TNR1 \begin{pmatrix} T_1 - T_{nom} \\ \bullet \\ \bullet \end{pmatrix} + TNR2 \begin{pmatrix} (T_1 - T_{nom})^2 \\ \bullet \\ \bullet \end{pmatrix}. \quad (17)$$

The resulting TNR1 and TNR2 parameters are displayed in the parameter list located on the right side of the front panel by selecting on the "LINEAR EQUATIONS" button. The TRS1,

TRS2, and GAMMA parameters are extracted from Eq. (6) by using two different methods: (i) the Linear Equation Method as shown in the following equation:

$$
\begin{pmatrix} \frac{R(T_1)}{R(T_{nom})} \\ \bullet \\ \bullet \end{pmatrix} = \begin{pmatrix} \left(\frac{T_1}{T_{nom}}\right)^{GAMMA} \\ \bullet \\ \bullet \end{pmatrix} + TRS1 \begin{pmatrix} (T_1 - T_{nom}) \\ \bullet \\ \bullet \end{pmatrix} + TRS2 \begin{pmatrix} (T_1 - T_{nom})^2 \\ \bullet \\ \bullet \end{pmatrix} \quad (18)
$$

and (ii) the Gauss-Newton Algorithm [11]. The resulting TRS1, TRS2, and GAMMA parameters are displayed in the parameter list located on the right part of the front panel by selecting the "LINEAR EQUATIONS" button using (i) and the "GAUSS-NEWTON" button using (ii). Statistically speaking, in order to extract the temperature dependent coefficients or exponents using the above two methods, there have to be at least three sets of model parameters extracted at different temperatures. All the resulting model parameters are displayed in the parameter list on the upper right corner of the front panel by selecting on the "ACCEPT" button.
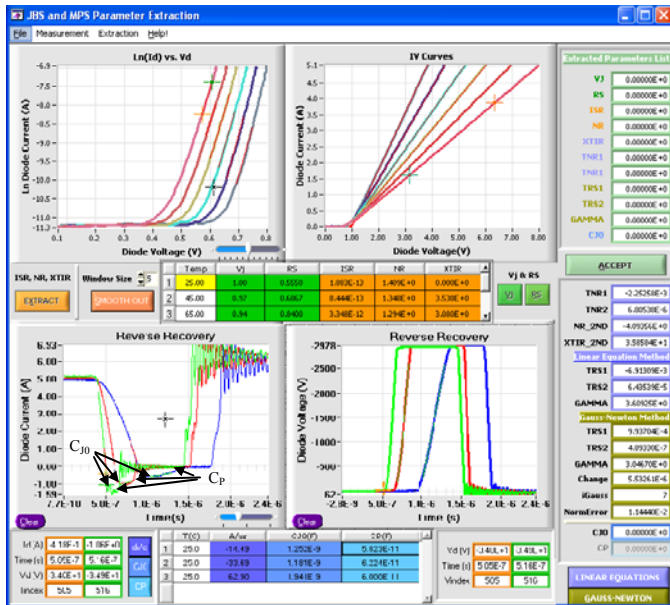


**Fig. 3** Sub-panel for extracting parameters from **Forward IV/Reverse Recovery** for Si and SiC JBS and MPS diodes.

*2).Reverse Recovery*

The bottom half of Fig. 3 was designed for the parameter extraction program of **Reverse Recovery**, which enables accurate model parameter extraction of $C_{J0}$ and $C_P$. The reverse recovery measurements are performed with different decreasing rates of the drive current (di/dt) to emulate the application conditions of different speed anti-parallel switching devices. The test system is well-characterized, meaning that the values of all circuit components and parasitic elements are known. The measured data are loaded and plotted in the bottom two graphs using the "File" pull-down window by selecting the "Load Single RR Curve" option from the "Load" submenu. The "di/c" button is used to extract the di/dt rate from the diode current waveforms (bottom-left) by aligning the two cursors on the current fall. The "CJ0" and

"CP" buttons are used to extract the capacitance values for $C_{J0}$ and $C_P$, respectively. Based on the discussion in subsection B of section II, the portions of the reverse recovery current waveform which are due to capacitances $C_{J0}$ and $C_P$ are pointed out in Fig. 3 (a) by arrows. The values for $C_{J0}$ and $C_P$ should be extracted such that the corresponding voltage waveforms (bottom-right) are aligned at the same time index and the correct dv/dt values are acquired.

*3).CV*

The capacitance-voltage (CV) measurement is the second method to extract $C_{J0}$ along with two other physical parameters: the built-in voltage ($V_{bi}$) and the drift region doping concentration ($N_d$). Fig. 4 shows the sub-panel of the parameter extraction program for the CV measurement, which is selected from the drop-down list in Fig. 2 (b). The measured CV data are loaded and then plotted in the graph on the left side of Fig. 4 using the "File" pull-down window and selecting the "Load" option. An internal function is called to calculate the reciprocal squared values of capacitance as shown in the form of

$$
\frac{1}{C^2} = \frac{2}{q N_d \varepsilon_r \varepsilon_0 A^2} (V_{bi} - V_A). \quad (19)
$$

The calculated values are plotted in the graph on the right side of Fig. 4. The "$C_{J0}$" button is used to extract the value for $C_{J0}$ by reading the capacitance value from the CV measurement under zero-biased condition. The "$V_{bi}$ & $N_d$" button is used to extract the values for $V_{bi}$ and $N_d$ which can be calculated from the x-intercept and the slope, respectively, as shown in (19). These two parameters will be used as device physical parameters in the **Reverse Leakage** program, which will be presented in subsection (4).
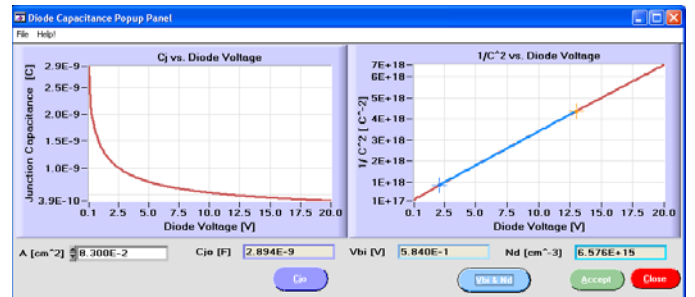


**Fig. 4** Sub-panel for extracting parameters from **CV** for Si and SiC JBS diodes.

*4).Reverse Leakage*

As discussed in Section II, a new physics-based model for the reverse leakage characteristics has been developed as an enhancement to the present power diode model in the Saber circuit simulator. Correspondingly, the newly derived model equations are implemented in DIMPACT for automatic parameter extraction. Fig. 5 shows the sub-panel of the parameter extraction program for the reverse leakage measurement which is selected from the drop-down list as shown in Fig. 2 (b).
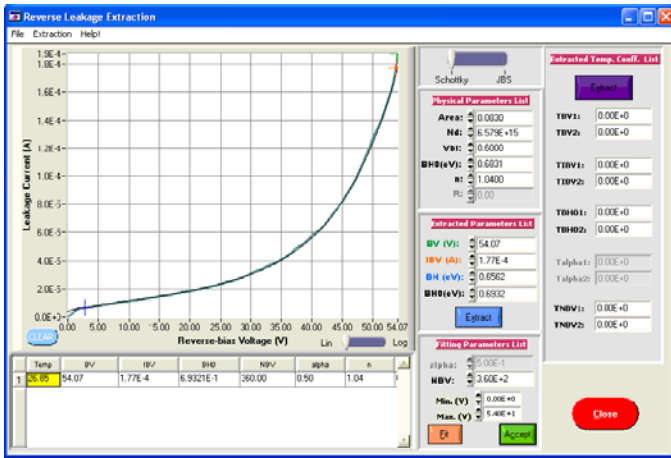
**Fig. 5** Sub-panel for extracting parameters from **Reverse Leakage** for Si and SiC JBS diodes.

This program enables the extraction of the parameters in the new model described in Section II including BV, $I_{BV}$, $N_{BV}$, $\phi_{B0}$, and $\alpha$, as well as the temperature coefficients for these parameters. Note that $\alpha$ and $R$ are model parameters used only for JBS diodes. A sliding bar is added next to the plotting area, which is used as an option to select the extraction between Schottky and JBS diodes. When the sliding bar is at "Schottky" position, the numerical controls for $\alpha$, $R$, $T\alpha 1$, and $T\alpha 2$ are dimmed. The extraction sequence also begins with the selection of the test fixture temperature and the material type of the power device. The input value for the test fixture temperature will be loaded into the table located at the bottom of the front-panel. The measured reverse leakage data are loaded and then plotted in the graph of Fig. 5 using the "File" pull-down menu by selecting the "Load" option. Physical and structural device parameters such as area (device active area), $N_d$, $V_{bi}$, and BH0 (zero-biased barrier height, or $\phi_{B0}$) are displayed in the numerical controls under the "Physical Parameter List" label because of their role in the calculation of model parameters as shown in equations (7) and (9). Note that the values for $N_d$ and $V_{bi}$ are extracted from the **CV** program as described in subsection (3); and the parameter BH0 displayed here is calculated from the saturation current extracted from the low-current range of the forward conduction measurement in the **Forward IV** program. Two cursors were activated to aid in the extraction process as shown in the graph of Fig. 5 where the blue cursor is enabled to extract the leakage current (y-axis value of the cursor) and the bias voltage (x-axis value of the cursor) in the very low-bias range; whereas the orange cursor is enabled to extract IBV and BV in the breakdown region. The leakage current extracted using the blue cursor is substituted into (7) to calculate the Schottky barrier height (BH or $\phi_B$) by assuming the impact ionization current is negligible when the bias is very low. The corresponding bias voltage extracted using the blue cursor is substitute into (8) to calculate the lowering effect of the Schottky barrier ($\Delta$BH, or $\Delta\phi_B$) which is then used to calculate BH0 by adding together with BH. The

"Extraction" button is used to read current and voltage values from the cursors, perform calculations as described above using an internal function, and display the extracted values for BV, IBV, BH, and BH0 into the numerical controls located under the "Extracted Parameters List" label. Notice that this program provides two methods of extracting the value for BH0: (i) from the forward-bias region and (ii) from the reverse-bias region. It offers an approach to verifying the accuracy of the extracted parameters by comparing the values for BH0 extracted separately using (i) and (ii).

The temperature-dependent coefficients are ready to be extracted after repeating the extraction procedure for each test fixture temperature. The "Extraction" button in purple is used to extract the values for TBV1, TBV2, TIBV1, TIBV2, TBH01, TBH02, TNBV1, TNBV2, Talpha1, and Talpha2 using the form of (14) and loading the extracted values into the numerical controls located under the "Extracted Temp. Coeff. List" label on the right side of the sub-panel.

### B. PiNMSR Program

By selecting "PINMSR" from the drop-down list as shown in Fig. 2 (a) and clicking the "RUN" button, a sub-panel as shown in Fig. 6 will pop-up for parameter extraction from measurements of **Forward IV** and **Reverse Recovery**. The model parameter extractions are performed in the sequence as described below.

#### 1). Forward IV

Fig. 6 shows the sub-panel of the parameter extraction program (**Forward IV/Reverse Recovery**) for PiN diodes, which is similar to the **Forward IV/Reverse Recovery** extraction sub-panel in the JBSMSR program but contains more model parameters. The top half of the sub-panel was designed for the parameter extraction program of **Forward IV**, which is capable of extracting all the model parameters used in the forward-bias region for PiN diodes including ISR, NR, XTIR, ISL, NL, XTIL, ISH, NH, XTIH, ISE, NE, XTIE, $V_J$, $R_S$, TNR1, TNR2, TNL1, TNL2, TNH1, TNH2, TNE1, TNE2, TRS1, TRS2 and GAMMA [5, 6]. These parameters are shown in the table located in the middle of the sub-panel as well as in the parameter list on the right half of the sub-panel in Fig. 6 as they are extracted.

The extraction sequence for PiN diodes is similar to the one used for Schottky/JBS diodes, which begins with the selection of the semiconductor material type as well as the test fixture temperature. Again, two commercial semiconductor curve tracers are used to aid in the parameter extraction process. The upper-left graph of Fig. 6 shows the diode current versus diode voltage on a logarithmic scale for the low-current range, which is used to extract parameters ISR, NR, and XTIR from the depletion region recombination range; and ISL, NL, and XTIL from the low-level injection range. The measured data are loaded and plotted in the graph using the "File" pull-down menu by selecting the "Load Low LN Curve" option from the "Load" submenu. The upper-right graph shows the diode current versus diode voltage for the high-current range, which is used to extract parameters ISH, NH, and XTIH from the high-level injection range; ISE, NE, and XTIE from the

emitter recombination range; and $V_J$ and $R_S$ from the series resistance range. Similarly, the measured data are loaded and plotted in the graph using the "File" pull-down menu by selecting the "Load single IV curve" option from the "Load" submenu. The top two graphs are for the test fixture temperature shown highlighted in the table. As described for the extraction techniques used in the JBSMSR program, the extraction is performed for each temperature first, and the extracted parameters are displayed in the table as shown in Fig. 6. The temperature coefficients and exponents are then extracted using two different methods: the Linear Equation and the Gauss-Newton Algorithm, which have been described in detail in the JBSMSR program. Finally, all the extracted parameters are displayed in the parameter list located on the right-side of the sub-panel as shown in Fig. 6.

### 2).Reverse Recovery

The bottom half of the sub-panel as shown in Fig. 6 is used for the parameter extraction program of **Reverse Recovery** for PiN diodes, which enables accurate model parameter extraction of $C_{J0}$, $C_P$, and three time-related parameters: TT, TSW, and TM due to the role of minority carriers in the intrinsic region as discussed in [5]. The reverse recovery measurements are performed using the same test system as the one used for Schottky/JBS diodes. The measured data are loaded and plotted in the bottom two graphs using the "File" pull-down menu by selecting the "Load Single RR Curve" option from the "Load" submenu. The buttons of "di/dt, CJ0, and CP" are used to extract the values for the di/dt rate, $C_{J0}$ and $C_P$, respectively, in the same way as described in the JBSMSR program. The buttons of "TT, TSW, and TM" are used to extract the values for TT, TSW, and TM from the corresponding range as shown in Fig. 6. All the extracted values are displayed in the table located at the bottom of the sub-panel.
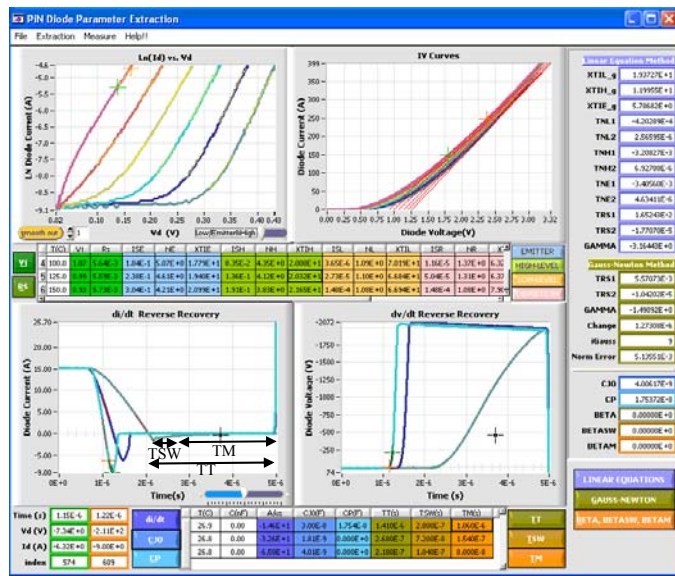


**Fig. 6** Sub-panel for extracting parameters from **Forward IV/Reverse Recovery** for Si and SiC PiN diodes.

## IV. MODEL PARAMETER VALIDATION

Figs. 7 to 10 show the comparison of measured (dashed) and simulated (solid) output characteristics over a temperature range from 25 °C to 150 °C for the 10 kV SiC JBS diode, the 10 kV SiC PiN diode, the 45 V Si Schottky diode, and the 600 V Si PiN diode, respectively. Fig. 11 shows the comparison of measured (red dashed) and simulated (black solid) junction capacitance for the 10 kV SiC JBS diode and the 45 V Si Schottky diode, respectively. Fig. 12 shows the comparison of measured (dashed) and simulated (solid) reverse blocking characteristics over a temperature range from 25 °C to 175 °C for the 10 kV SiC JBS diode. Figs. 13 and 14 show the comparison of measured (dashed) and simulated (solid) reverse recovery at 25 °C for the 10 kV SiC JBS diode and the 10 kV SiC PiN diode, respectively.

## V. CONCLUSION

This paper presents a software program for model parameter extraction called DIMPACT which consists of three programs: JBSMSR, MPSMSR, and PiNMSR. The program provides a method to automatically extract model parameter sets and rapidly construct power diode models for JBS, MPS, and PiN diodes. The diodes that were studied in this paper include a 45V Si Schottky diode, a 10 kV SiC JBS diode, a 600 V Si PiN diode, and a 10 kV SiC PiN diode. The validation results are demonstrated for the static conduction characteristics and the transient characteristics in the Saber circuit simulator, which prove the accuracy of the model parameters extracted using DIMPACT. This software package currently is not available for public download.

### REFERENCES

[1] R. Singh, S. Ryu, J. Palmer, A. Hefner, J. Lai, "1500 V, 4 Amp 4H-SiC JBD Diodes," Proceedings of the 2000 International Symposium on Power Semiconductor Devices and ICs, May 2000, pp. 101-104.
[2] B. Hull, J. Sumakeris, M. O' Loughlin, Q Zhang, J. Richmond, A. Powell, E. Imhoff, K. Hobart, A Rivera-Lopez, and A. Hefner, Jr., " Performance and Stability of Large-Area 4H-SiC 10-kV Junction Barrier Schottky Rectifiers," *IEEE Transactions on Electron Devices*, **55**, 2008, 1864-1870.
[3] A. Hefner, "Performance Analysis of 10 kV, 100 A SiC Half-Bridge Power Modules," Proceedings of the Government Microcircuit Applications and Critical Technology Conference (GOMACTech) 2008, March 17-20, 2008, Las Vegas, NV, pp. 361-364.
[4] P. Sun; J. Lai, H. Qian, We. Yu, C. Smith, J. Bates, "High Efficiency Three-phase Soft-switching Inverter for Electric Vehicle Drives," Vehicle Power and Propulsion Conference, 2009. VPPC '09. IEEE, pp. 761-766.
[5] T. R. McNutt, A. R. Hefner, H. A. Mantooth, J. L. Duliere, D. W. Beming, and R. Singh, "Parameter Extraction Sequence for Silicon Carbide Schottky, Merged PiN Schottky, and PiN Power Diode Models," IEEE, 2002, pp. 1269-1276.
[6] T. R. McNutt, A. Hefner, Jr., H. Mantooth, J. Duliere, D. Berning, and R. Singh, "Silicon Carbide PiN and Merged PiN Schottky Power Diode Models Implemented in the Saber Circuit Simulator," *IEEE Trans. Power Electron.*, vol. 19, no. 3, pp. 573-581, 2004.
[7] H. Mantooth, J. Duliere, "A unified diode model for circuit simulation," *IEEE Trans. Power Electron.*, vol. 12, no. 5, pp. 816-823, 1997.
[8] The MathWorks, Inc.
[9] S. M. Sze, *Physics of Semiconductor Devices*, WILEY_INTESCIENCE Publishing, 2007.
[10] L. Zhu, T. Chow, " Analytical Modeling of High-Voltage 4H-SiC Junction Barrier Schottky (JBS) Rectifiers," *IEEE TRANSACTION Transactions on Electron Devices*, VOL. **55**, NO.8 p1857-1863, 2008.
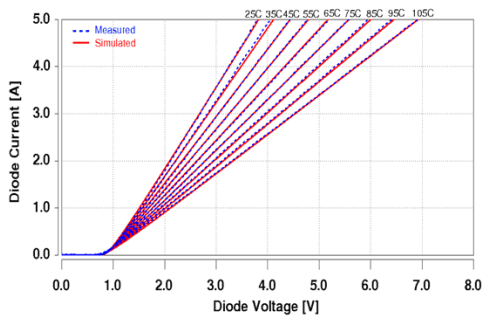[11] G. A. F. Seber and C. J. Wild, *Nonlinear Regression*, Hoboken, NJ: John Wiley & Sons, Inc., 2003.

**Fig. 7:** Comparison of measured (dashed) and simulated (solid) output characteristics at 25 °C, 35 °C, 45 °C, 55 °C, 65 °C, 75 °C, 85 °C, 95 °C and 105 °C for a 10 kV, 5 A SiC JBS diode.
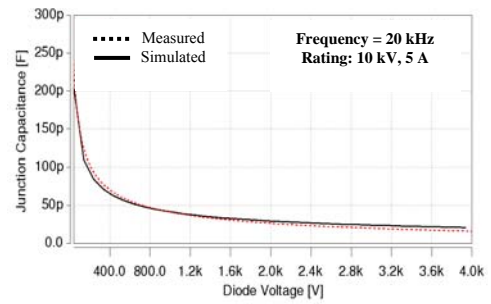


**Fig. 11:** Comparison of measured (red dashed) and simulated (black solid) junction capacitance for a 10 kV, 5 A SiC JBS diode.
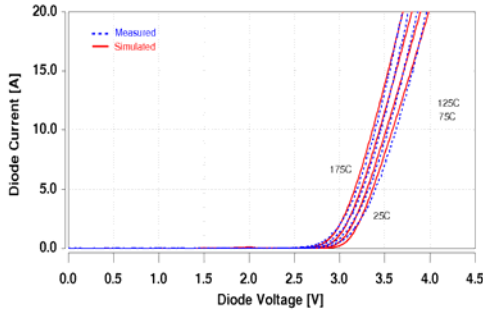


**Fig. 8:** Comparison of measured (dashed) and simulated (solid) output characteristics at 25 °C, 75 °C, 125 °C and 175 °C for a 10 kV, 20 A SiC PiN diode.
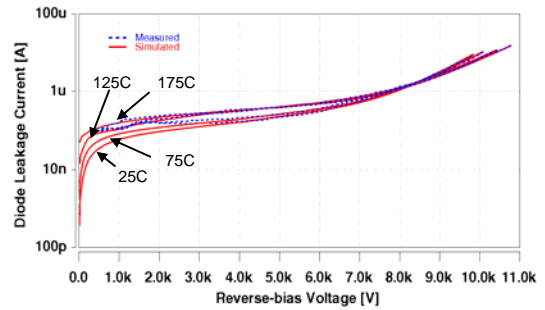


**Fig. 12:** Measured (dashed) and simulated (solid) reverse-biased leakage for a 10 kV, 5 A SiC JBS diode in log scale at 25 °C, 75 °C, 125 °C, and 175 °C.
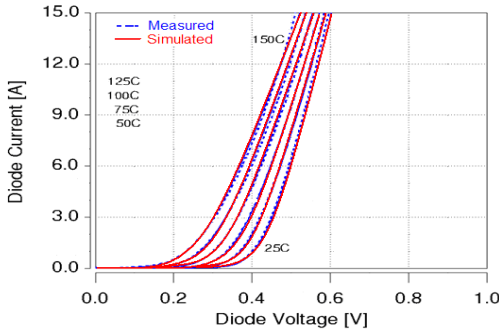


**Fig. 9:** Comparison of measured (dashed) and simulated (solid) output characteristics at 25 °C, 50 °C, 75 °C, 100 °C, 125 °C, and 150 °C for a 45 V, 15 A Si Schottky diode.
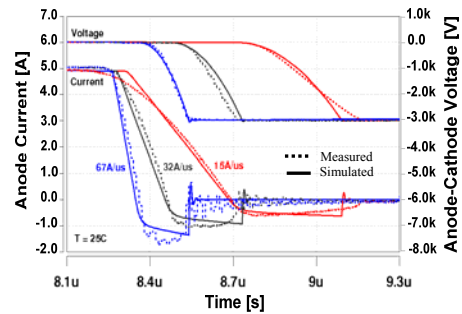


**Fig. 13:** Comparison of measured (dashed) and simulated (solid) reverse recovery at 25 °C for a 10 kV, 5 A SiC JBS diode.
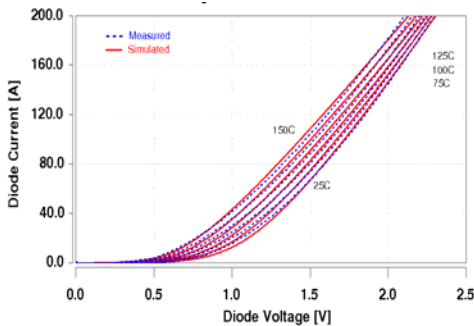


**Fig. 10**: Comparison of measured (dashed) and simulated (solid) output characteristics at 25 °C, 50 °C, 75 °C, 100 °C, 125 °C, and 150 °C for a 600 V, 200 A Si PiN diode.
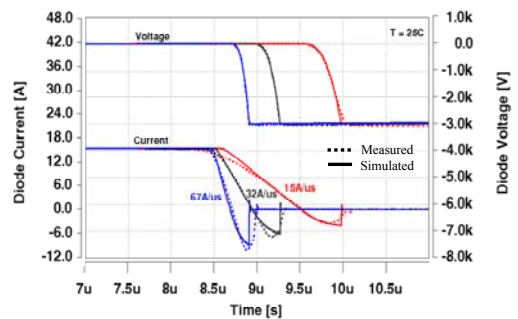


**Fig. 14:** Comparison of measured (dashed) and simulated (solid) reverse recovery at 25 °C for a 10 kV, 20 A SiC PiN diode.